APPLIED AND ENVIRONMENTAL MICROBIOLOGY, Apr. 2009, p. 2111–2121 Vol. 75, No. 7
0099-2240/09/$08.00+0 doi:10.1128/AEM.01540-08

Dynamics of Polyphosphate-Accumulating Bacteria in Wastewater Treatment Plant Microbial Communities Detected via DAPI (4′,6′-Diamidino-2-Phenylindole) and Tetracycline Labeling▽†

S. Günther,[1] M. Trutnau,[2] S. Kleinsteuber,[1] G. Hause,[3] T. Bley,[2] I. Röske,[4] H. Harms,[1] and S. Müller[1]*

Department of Environmental Microbiology, UFZ-Helmholtz Centre for Environmental Research, Permoserstrasse 15, 04318 Leipzig, Germany[1]; Institute of Food Technology and Bioprocess Engineering, Dresden University of Technology, Bergstrasse 120, 01069 Dresden, Germany[2]; Microscopy Unit, Biocenter of the University Halle-Wittenberg, Weinbergweg 22, 06120 Halle/Saale, Germany[3]; and Institute of Microbiology, Dresden University of Technology, Zellescher Weg 20b, 01217 Dresden, Germany[4]

Received 8 July 2008/Accepted 15 January 2009

Wastewater treatment plants with enhanced biological phosphorus removal represent a state-of-the-art technology. Nevertheless, the process of phosphate removal is prone to occasional failure. One reason is the lack of knowledge about the structure and function of the bacterial communities involved. Most of the bacteria are still not cultivable, and their functions during the wastewater treatment process are therefore unknown or subject of speculation. Here, flow cytometry was used to identify bacteria capable of polyphosphate accumulation within highly diverse communities. A novel fluorescent staining technique for the quantitative detection of polyphosphate granules on the cellular level was developed. It uses the bright green fluorescence of the antibiotic tetracycline when it complexes the divalent cations acting as a countercharge in polyphosphate granules. The dynamics of cellular DNA contents and cell sizes as growth indicators were determined in parallel to detect the most active polyphosphate-accumulating individuals/subcommunities and to determine their phylogenetic affiliation upon cell sorting. Phylotypes known as polyphosphate-accumulating organisms, such as a "*Candidatus* Accumulibacter"-like phylotype, were found, as well as members of the genera *Pseudomonas* and *Tetrasphaera*. The new method allows fast and convenient monitoring of the growth and polyphosphate accumulation dynamics of not-yet-cultivated bacteria in wastewater bacterial communities.

Enhanced biological phosphorus removal (EBPR) is a widely implemented technique for phosphate removal in wastewater treatment processes, since it is economical while being more environmentally friendly than the traditional chemical treatment (10). Unfortunately, despite several years of intensive research into phosphorus-accumulating organisms (PAOs), the EBPR process is unstable. Moreover, many pure cultures, e.g., members of the genera *Acinetobacter*, *Microlunatus*, *Tetrasphaera*, and *Lampropedia*, have been isolated, which showed traits expected from PAOs, but none of them were found to have great significance in wastewater treatment plants (WWTPs) (8, 33, 35, 44). Our knowledge of PAOs that are active in WWTPs is therefore cursory at best, and it has been suggested that bacterial species which are not yet cultivated may be responsible for the polyphosphate accumulation (16). Monitoring of these organisms thus requires cultivation-independent techniques directed at specific characteristics of PAOs, such as the accumulated polyphosphate. For the selective analysis of PAOs within complex communities, single-cell-based methods such as fluorescence microscopy and flow cytometry appear to be most appropriate.

Polyphosphate granules were first identified in *Saccharomyces cerevisiae* in 1888 (24). Since then, the ability to store polyphosphates as granules within the cell was found to be widespread among microorganisms. The inert polymers fulfill various functions (for a review, see reference 21). They consist of linear orthophosphate chains ranging from few to several hundred residues which are linked by energy-rich phosphoanhydride bonds. As polyanions, the polyphosphate chains need counterions to neutralize the negative charge. The most important counterions are Mg^{2+}, Ca^{2+}, and K^{+}. Several other cations, such as Mn^{2+}, Al^{3+}, and Fe^{3+}, were found to be incorporated to a lesser extent, depending on the growth conditions and microorganisms under investigation (42). Currently, polyphosphate accumulation is studied by bulk measurements such as ^{31}P nuclear magnetic resonance analysis (31) or even more frequently by quantifying the activity of the polyphosphate kinase (Ppk) (4). Single-cell approaches also have been applied for a long time, with examples being phase-contrast or bright-field microscopy. Neisser's staining and Loeffler's methylene blue are the traditional nonfluorescent stains for microscopic analysis of PAOs (34). Electron microscopic analysis made use of labeled antibodies to facilitate the detection of phosphate granules (32). Another compound that is widely used to visualize polyphosphate granules is the fluorescent dye 4′,6′-diamidino-2-phenylindole (DAPI) (41), which stains cells with polyphosphate contents higher than 400 μmol g^{-1} (dry weight) when applied at a concentration of at least 18 μM (5 to 50 μg ml^{-1}) *18, 40). DAPI staining depends on a polyphosphate-mediated metachromatic reaction which

* Corresponding author. Mailing address: UFZ-Helmholtz Centre for Environmental Research Leipzig-Halle, Department of Environmental Microbiology, Permoserstrasse 15, 04318 Leipzig, Germany. Phone: 49 341 235 1318. Fax: 49 341 235 1351. E-mail: susann.mueller@ufz.de.

† Supplemental material for this article may be found at http://aem.asm.org/.

▽ Published ahead of print on 30 January 2009.

TABLE 1. Bacterial species used in this study

Organism	Source	Rationale for usage
Microlunatus phosphovorus NM-1 (DSM 10555)	German Collection of Microorganisms and Cell Cultures	Model organism for polyphosphate production
Pseudomonas sp.	Wastewater isolate (M. Eschenhagen, Dresden University of Technology, Germany)	Model organism for polyphosphate production
Paracoccus sp.	Wastewater isolate (M. Eschenhagen, Dresden University of Technology, Germany)	Model organism for polyphosphate production
Escherichia coli K-12	UFZ strain collection	Negative control (DNA binding of TC)
Methylobacterium rhodesianum MB126	UFZ strain collection	Negative control (PHB binding of TC)
Micropruina glycogenica Lg2^T (DSM 15918)	German Collection of Microorganisms and Cell Cultures	Negative control (glycogen binding of TC)

causes a shift in the emitted fluorescence from blue to a bright yellow-green. When DAPI is applied at lower concentrations (0.24 to 5 μM), the resulting blue fluorescence is related to bacterial DNA. Unfortunately, unspecific fluorescence of other cellular constituents such as lipids also was reported when DAPI was applied at high concentrations (180 μM) (40). Another, but not commonly used, fluorescent dye is 9-aminoacridine, which has properties similar to those of DAPI as it emits blue fluorescence when binding to DNA and green fluorescence when binding to polyphosphate granules (21).

Individual-based fluorescent techniques can be used to detect bacteria in natural communities which are able to synthesize polyphosphates but cannot be grown in pure culture. Particularly promising is the recognition of PAOs by flow cytometry in combination with cell sorting for further phylogenetic identification, an approach to be presented in this report. A few applications of flow cytometry to determine polyphosphate granules have been reported. They involved DAPI alone (46) or in combination with fluorescence in situ hybridization (FISH) (16). However, the aforementioned unspecific DAPI staining may spoil the quantitative and possibly even the qualitative determination of PAOs in natural communities.

The fluorescent antibiotic tetracycline (TC) and its derivatives are frequently used in medicine as a label for calcium deposition in bone or teeth and as a marker for membrane-associated divalent cations (12). The binding mode is still unclear, although several mechanisms have been discussed (for a review, see reference 27). When TC is bound to diamagnetic divalent cations such as calcium and magnesium, its fluorescence intensity is enhanced, with excitation and emission maxima at 390 nm and 515 nm, respectively (at pH 7.5) (23). Using this effect, we developed a new fluorescence technique that makes use of the interaction of TC hydrochloride with countercations of polyphosphate granules and can be used for the quantitative determination of polyphosphate in individual bacterial cells.

Here we present the development of a dual polyphosphate/DNA fluorescent staining approach and its application to follow PAO dynamics within natural communities. Representative PAOs were isolated by cell sorting and identified by sequencing and terminal restriction fragment length polymorphism (T-RFLP) profiling of 16S rRNA genes. This mining of not-yet-cultivable PAOs from wastewater samples greatly increases our knowledge of genuine polyphosphate accumulators in an EBPR process and will open options for knowledge-based optimization of WWTPs.

MATERIALS AND METHODS

Bacterial strains and culture conditions. The bacterial strains used in this study are shown in Table 1. Cells were cultivated in 500-ml shake flasks with tightly closed screw caps at 150 rpm and 30°C in 100 ml of the synthetic wastewater described by Hrenovic et al. (14). They were subjected to alternating aerobic and anaerobic conditions (changing every 12 h). For every new anaerobic process interval, the medium was replenished with 0.26 mM propionate, 0.1 g liter^{-1} peptone, and 54 μM $CaCl_2$ as well as 83 μM $MgSO_4$ and 1.6 mM KH_2PO_4. To establish aerobic and anaerobic conditions, the culture was flushed with sterile air and with sterile nitrogen of highest purity, respectively, for at least 60 min.

Escherichia coli and the non-polyphosphate-producing *Micropruina glycogenica* (37) were grown aerobically in 300-ml shake flasks in 50 ml peptone medium containing (per liter) 5 g peptone from meat (pancreatic), 3 g NaCl, 2 g K_2HPO_4, 10 g meat extract, 10 g yeast extract, and 5 g glucose (for *E. coli*) and in DSM 776 for *M. glycogenica*. *Methylobacterium rhodesianum* was grown aerobically in 100-ml shake flasks in 50 ml of the standard medium described by Ackermann et al. (1). This strain was reported to produce poly-β-hydroxybutyrate (PHB) to up to 95% of its dry weight. Methanol (120 mM) was added as a carbon and energy source. The three control strains were cultivated at 30°C, 150 rpm, and pH 7.0. Cultures were checked regularly for purity by streaking aliquots on agar plates of the respective medium (given above) as well as microscopic observation.

Reactor operation. Activated sludge was harvested from one aeration tank of the Elsterwerda WWTP (Brandenburg, Germany) and cultivated in a 7-liter laboratory bioreactor with a working volume of 5 liters (New Brunswick BioFlow III; New Brunswick Scientific) (see Fig. S1 in the supplemental material) at 300 rpm (except for the settling period) and 20°C. The pH value of 7 ± 0.05 was automatically regulated by titration with either 0.6 M HCl or 0.5 M NaOH. The reactor was operated as sequenced-batch reactor (SBR) with a cycle time of 6 h four times a day, consisting of an aerobic period (2 h, aerated) followed by a settling and refilling period for restoring anaerobic conditions (2 h, manual feed) and an anaerobic period (2 h). The initial mixed-liquor suspended solids (MLSS) were set to 2.5 g liter^{-1} by appropriate dilution with cultivation medium (OECD synthetic wastewater) containing (per liter) 0.16 g peptone from meat (pancreatic), 0.11 g meat extract, 0.03 g urea, 0.028 g KH_2PO_4, 0.007 g NaCl, 0.004 g $CaCl_2 \cdot 2H_2O$, and 0.002 g $MgSO_4 \cdot 7H_2O$. Trace elements (2 ml liter^{-1}) were added as a solution containing (per liter) 0.07 g $ZnCl_2$, 0.1 g $MnCl_2 \cdot 4H_2O$, 0.2 g $CoCl_2 \cdot 6H_2O$, 0.1 g $NiCl_2 \cdot 6H_2O$, 0.02 g $CuCl_2 \cdot 2H_2O$, 0.05 g $NaMoO_4 \cdot 2H_2O$, 0.026 g $Na_2SeO_3 \cdot 5H_2O$, and 1 ml 25% HCl. For overnight SBR operation, settling and refilling were replaced by automated feeding of concentrated medium (43 ml/6 h) to result in a final concentration equal to that from the manual feed. The concentrations of phosphate and other components of the medium were changed during the cultivation as indicated according to the demands of the experiments. The oxygen was recorded by an oxygen sensor (Applicon, The Netherlands). The pH was analyzed with a sensor from Mettler-Toledo (Switzerland). Inorganic phosphate and nitrate were measured by ion chromatography (IC) (Dionex Corporation). IC analysis was performed on a DX 320 IC with an EG40 eluent generator and an IonPac NG1 guard column (4 by 35 mm) connected to an IonPac AS15 (4 mm) separation column. The separation was obtained at a flow rate of 0.4 ml min^{-1} with a gradient program (KOH and water) rising from 5 mM to 30 mM in the first 7 min and to 45 mM in the next 10 min. The concentration of KOH then was kept constant for 5 min and finally decreased to 5 mM within 2 min. MLSS values (g total suspended solids liter^{-1}), mixed-liquor volatile suspended solids (MLVSS) values (g volatile suspended

solids liter^{-1}), chemical oxygen demand (COD) values (mg liter^{-1}) (7), and ash contents (g liter^{-1}) were determined using standard methods (9a).

Cell preparation. Cells of *Microlunatus phosphovorus*, a *Pseudomonas* sp., and a *Paracoccus* sp. were harvested according to the demands of the experiments. *E. coli*, *M. glycogenica*, and *M. rhodesianum* were harvested at the stationary phase of growth. The samples were washed twice with phosphate-buffered saline (PBS) (0.4 M Na_2HPO_4/NaH_2PO_4, 150 mM NaCl, pH 7.2) to remove any disturbing substances (cell debris or organic material) by centrifugation at 3,200 × *g* for 5 min (10 min for activated sludge samples) and conserved in fixation buffer (pH 7.0) containing 5 mM $BaCl_2$ ($BaCl_2 \cdot 2H_2O$; Laborchemie Apolda, Germany), 5 mM $NiCl_2$ ($NiCl_2 \cdot 6H_2O$; Merck, Germany), and 10% sodium azide (Merck, Germany) dissolved in PBS (1 ml fixation buffer for approximately 3×10^8 cells ml^{-1}) as described by Günther et al. (11) for a maximum of 9 days. For further information on cell preparation, see reference 11.

Staining procedures and flow cytometry. (i) DNA. DNA staining was done as described previously (11), using a variation of a standard procedure (25). A DAPI solution of 0.24 μM was used for DNA staining of activated sludge samples, and a 1 μM solution was used for *M. phosphovorus*.

(ii) Polyphosphates. For cellular polyphosphate staining, two different dyes were applied. The first one was DAPI, which is known to stain polyphosphates at high concentrations. Two milliliters of adjusted cell suspension was centrifuged and treated with 1 ml solution A for 20 min. The cells were then washed and resuspended carefully in 2 ml of a 28 μM DAPI stock solution.

The second dye was the antibiotic TC hydrochloride (Fluka, Switzerland). It was applied as a 2-mg ml^{-1} stock solution in double-distilled water to give a final concentration of 0.225 mM in the cell suspension. Stock solutions were prepared freshly before each experiment to prevent low data quality due to TC aging. The dramatic decline in fluorescence intensity of the TC stock solution after storage for only 3 days in a refrigerator is presented in the inset of Fig. S2 in the supplemental material. The stained samples were stored for 60 min at 20°C in the dark before flow cytometric measurement. For the experiments with activated sludge, unstained cells served as controls. The number of cells displaying strong green autofluorescence was subtracted from the fluorescence counts obtained from TC-stained samples to obtain polyphosphate-related fluorescence information (see also the description of the gating strategy below).

(iii) DNA and polyphosphates. For dual staining of the DNA and polyphosphate granules by DAPI and TC, the cells were first subjected to solution A for 20 min, centrifuged, washed, and treated with 0.225 mM TC for 10 min before 2 ml solution B (0.24 μM and 1 μM for activated sludge and *M. phosphovorus*, respectively) was added. Stained samples were incubated for another 60 min at 20°C in the dark before flow cytometric measurement.

(iv) PHB. To visualize cellular PHB contents, Nile red (Sigma) was applied as described previously (1).

(v) Scatter behavior. Forward scatter (FSC) is related to cell size, and side scatter (SSC) is related to cell granularity. Data were obtained by examining the light-scattering behavior of individual cells, mediated by the 488-nm line of the argon ion laser. Usually, shifts in the FSC/SSC mean values were recorded in parallel with the fluorescence measurements.

(vi) Flow cytometry. Analyses were carried out using a MoFlo cell sorter (DakoCytomation) equipped with two water-cooled argon-ion lasers (Innova 90C and Innova 70C from Coherent). Excitation of 400 mW at 488 nm was used to analyze the Nile red fluorescence, FSC, and SSC at the first observation point. SSC was used as a trigger signal to discriminate bacterial cells from electronic noise. DAPI and TC were excited by 100 mW of multiline ultraviolet (333 to 365 nm) at the second observation point. The orthogonal signal was first reflected by a beam splitter and then recorded after reflection by a 555-nm long-pass dichroic mirror and passage by a 505-nm short-pass dichroic mirror and a 488/10 band-pass (BP) filter. Blue (DAPI) fluorescence was passed through a 450/65 BP filter, green (TC and DAPI) fluorescence through a 520/15 BP filter, and red (Nile red) fluorescence through a 620/45 BP filter. Photomultiplier tubes were obtained from Hamamatsu Photonics (models R 928 and R 3896; Hamamatsu, Japan). Amplification was carried out at logarithmic scales for all measurements. Tuning of the device was done as described by Kleinsteuber et al. (19).

Sorting of TC-stained, polyphosphate-containing bacterial cells was done using the most accurate sort mode (single and one-drop mode; highest purity, 99%) at a rate not higher than 1,500 cells per second. Cell sorting was performed using the four-way sort option at high speed (12 ms^{-1}). The cells were sorted into nucleic acid-free glass flasks. Cells were separated from the mixed culture using TC-polyphosphate fluorescence intensity and FSC signals in several independent experiments using different gate settings (see Fig. S3 in the supplemental material). Polyphosphate-containing subcommunities were separated by sorting in order to facilitate their phylogenetic identification. To obtain sufficient DNA for the generation of 16S rRNA gene clone libraries, at least 10^6 cells were sorted.

(vii) Data evaluation. The acquired data were analyzed as described by Günther et al. (11). The sort gates were placed around particularly abundant or distinct, rare subcommunities according to similarity in fluorescence and size properties. The data were determined from two independent experiments analyzed in two parallels each.

Fluorescence microscopy. To verify reliable staining and purity and to inspect cell morphologies, the cells were subjected to microscopy and image analysis (Axioskop [Zeiss] microscope, DXC-9100P camera, and Openlab 3.1.4. [Improvision] software) using light from a 100-W mercury arc lamp. The Zeiss filter set 02 (excitation G 365, BS 395, emission LP 420) was used for examining blue fluorescence of DAPI-stained cells as well as green fluorescence of TC (0.225 mM)- or DAPI (28 μM)-stained PAO cells. Red fluorescence from Nile red-stained cells (PHB detection) was observed using the Zeiss filter set 15 (excitation 546/12, BS 580, emission LP 590). For better visualization of cell properties, phase-contrast and fluorescence images were merged using the Openlab software.

TEM. For transmission electron microscopy (TEM), the cells were fixed with 3% glutaraldehyde (Sigma, Germany) in 0.1 M sodium cacodylate buffer (SCB) (pH 7.2) for 1 h at 20°C. Thereafter the cells were immobilized with 4% agar (Roth, Germany) in SCB and thoroughly washed four times with SCB. Polyphosphate staining was done as described by Jensen (15). Instead of a 20% $Pb(NO_3)_2$ solution, a 2% $Pb(NO_3)_2$ solution was used. Samples were dehydrated in a graded ethanol series and embedded in epoxy resin (39). Ultrathin sections (80 nm) were transferred to Formvar-coated copper grids and examined without further staining using an EM 900 transmission electron microscope (Zeiss SMT, Germany) at an acceleration voltage of 80 kV. Electron micrographs were taken with a slow-scan camera (Variospeed slow-scan charge-coupled device camera SM-1k-120; TRS, Germany). The size of the polyphosphate particles was determined using the iTEM software (Olympus SIS, Germany).

Fluorescence spectra. The fluorescence spectrum of TC hydrochloride (dissolved in PBS, 2.25 mM final concentration) was analyzed using the scan mode of an LS-50B luminescence spectrometer (Perkin-Elmer). The following settings were used to get information on the fluorescent properties of the compound when excited at 365 nm, which is the highest excitation wavelength of the multiline-ultraviolet argon-ion laser of the MoFlo used for single cell analysis: emission, 300 to 600 nm; number of scans, 2; excitation and emission slit, 10; and scan speed, 240 nm min^{-1}. The emission spectrum of pure TC without divalent cations is given in Fig. S2 in the supplemental material. To evaluate the fluorescence properties of cells stained with TC, the same instrument settings were chosen and the front surface accessory option of the Perkin-Elmer device was used to analyze fluorescence in cell suspensions. Activated sludge cells harvested from the aerobic cultivation phase and fixed for 1 day were washed twice and resuspended in PBS to yield an optical density of 0.1. The cells were stained with 0.225 mM TC (final concentration) and analyzed (see Fig. S2 in the supplemental material). An unstained cell suspension served as a control (see Fig. S2 in the supplemental material). The peaks at 365 nm are the excitation peaks of the respective samples.

Pure dissolved TC hydrochloride solution showed a very low fluorescence maximum at 515 nm, with the respective fluorescence intensity around 0.2. Unstained cells exhibited a fluorescence peak at between 415 and 420 nm and no fluorescence above the background level at 515 nm (fluorescence intensity of about 1.0). TC stained cell suspensions exhibited a small emission shoulder at 420 nm and a large peak with a maximum at 515 nm. The relative fluorescence intensity of about 10 was 50 times above that of TC solution in PBS and 10 times higher than the background level of unstained cell suspension.

DNA preparation, 16S rRNA gene cloning, and sequencing. For preparation of genomic DNA, sorted cells were harvested from the sheath buffer by centrifugation and resuspended in 10 μl 10 mM Tris-HCl, pH 9.0. Cells were disrupted by a 10-min microwave treatment at 95°C in a BP-111-RS-IR thermostat microwave device (Microwave Research and Applications Inc.), immediately chilled on ice for 10 min, and then centrifuged for 10 min at 23,100 × *g* and 4°C. From the supernatant, bacterial 16S rRNA gene fragments were amplified by PCR using the universal primers 27F and 1492R (22). PCR was performed in a 12.5-μl reaction mixture containing 6.25 μl *Taq* PCR master mix (Qiagen, Germany), 5 pmol of each primer (supplied by Microsynth, Switzerland), and 4 μl template DNA with a PTC-200 thermal cycler (MJ Research, USA). For the cycle parameters and cloning strategy, see reference 19. Positive clones were screened by double digestion with the restriction enzymes HaeIII and RsaI (New England Biolabs, Germany). Partial DNA sequencing of representative clones displaying different restriction patterns was performed with the BigDye RR Terminator AmpliTaq FS Kit 1.1 (Applied Biosystems, Germany) and the sequencing primers 27F and 519R (22). Capillary electrophoresis and data collection were carried out on an ABI Prism 3100 genetic analyzer (Applied Biosystems). Data were

analyzed with ABI Prism DNA sequencing analysis software, and 16S rRNA gene sequences were assembled using Sequencher 4.8 (Gene Codes Corp.). The BLASTN tool (www.ncbi.nlm.nih.gov/BLAST) (3) was used to search for similar sequences in the GenBank database, and the Seqmatch tool was used to search for similar sequences compiled by the Ribosomal Database Project (RDP) release 10.0 beta (http://rdp.cme.msu.edu) (9).

T-RFLP analyses. Bacterial 16S rRNA gene fragments were PCR amplified with the primers 27F-FAM (labeled at the 5′ end with phosphoramidite fluorochrome 5-carboxyfluorescein) and 1492R (22). Labeled oligonucleotides were purchased from biomers.net (Germany). PCR was performed as described above. PCR products were purified using the Wizard SV PCR clean-up system (Promega, Germany) and quantified after agarose gel electrophoresis and ethidium bromide staining using the GeneTools program (Syngene, United Kingdom). Purified PCR products were digested with the restriction endonuclease AluI, HaeIII, or Sau3AI (New England Biolabs, Germany). A 10-μl reaction mixture contained 1 ng DNA (for T-RFLP analyses of single clones) or 20 ng DNA (for T-RFLP analyses of the entire sample of sorted cells) and 10 units of restriction enzyme. Samples were incubated at the appropriate temperature for 3 h and then precipitated with sodium acetate (pH 5.5) and ethanol. Dried DNA samples were resuspended in 20 μl HiDi formamide containing 1.5% (vol/vol) GeneScan-500 ROX standard (Applied Biosystems). Samples were denatured at 95°C for 5 min and chilled on ice. The fragments were separated by capillary electrophoresis on an ABI Prism 3100 genetic analyzer (Applied Biosystems). The lengths of the fluorescent terminal restriction fragments (T-RF) were determined using the GeneMapper V3.7 software (Applied Biosystems), and their relative peak areas were determined by dividing the individual T-RF area by the total area of peaks within the threshold of 35 to 650 bp. Only peaks with relative fluorescence intensities of at least 20 units were included in the analysis. Theoretical T-RF values of the dominant phylotypes represented in the clone library were calculated using the NEB cutter (http://tools.neb.com/NEBcutter2/index.php) and confirmed experimentally by T-RFLP analysis using the corresponding clones as templates. Relative T-RF abundances of representative phylotypes were determined based on the relative peak areas of the corresponding T-RF.

Nucleotide sequence accession numbers. The 16S rRNA gene sequences determined in this study have been deposited in the GenBank database under accession numbers EU850352 to EU850394.

RESULTS

Optimization of TC staining of polyphosphate. The TC staining procedure was optimized with *M. phosphovorus* NM-1 and a bacterial community derived from activated sludge of the SBR. Influences of incubation times (0 to 180 min) and TC concentrations (0.023 to 1.35 mM) on staining results were tested (see Fig. S4 in the supplemental material). This was necessary to minimize unspecific staining or dye interactions as a prerequisite for obtaining quantitative information on individual polyphosphate contents. Good results were obtained after 10 min of exposure to 0.225 mM TC. As the staining was stable in fixed as well as living samples for 3 h, there was no sign of efflux pumping of TC.

Polyphosphate staining in pure cultures. Green fluorescent polyphosphate granules were detected and quantified by flow cytometry (see below) and fluorescence microscopy (Fig. 1a to d). Granules were clearly visible in *M. phosphovorus*, *Pseudomona*s spp., and *Paracoccus* spp., all harvested after 3 days of alternating aerobic/anaerobic shifts at the end of an aerobic phase. The distribution, amount, and size of the polyphosphate granules varied among the strains as analyzed and observed by both fluorescence microscopy and TEM (Fig. 1e). Within these samples the granule diameters varied between 0.25 and 1.33 μm, with average sizes of 0.69 μm for *M. phosphovorus*, 0.48 μm for the *Pseudomona*s sp., and 0.39 μm for the *Paracoccus* sp. (average of 17 granules each). The sizes of the granules in *M. phosphovorus* (Fig. 1e) and the *Pseudomonas* sp. obtained by fluorescence microscopy were verified by TEM (average of 100 granules each). The granule sizes measured by TEM were significantly lower. *M. phosphovorus* showed granule sizes varying from 0.52 to 0.08 μm with an average size of 0.26 μm (±0.10 μm), and the *Pseudomona*s sp. showed granule sizes varying from 0.17 to 0.04 μm with an average size of 0.10 μm (±0.03 μm). The differences between results with the two technologies may partly be an artifact of epifluorescence-based sizing and the spatial position of the granule within the 80-nm slices analyzed by TEM.

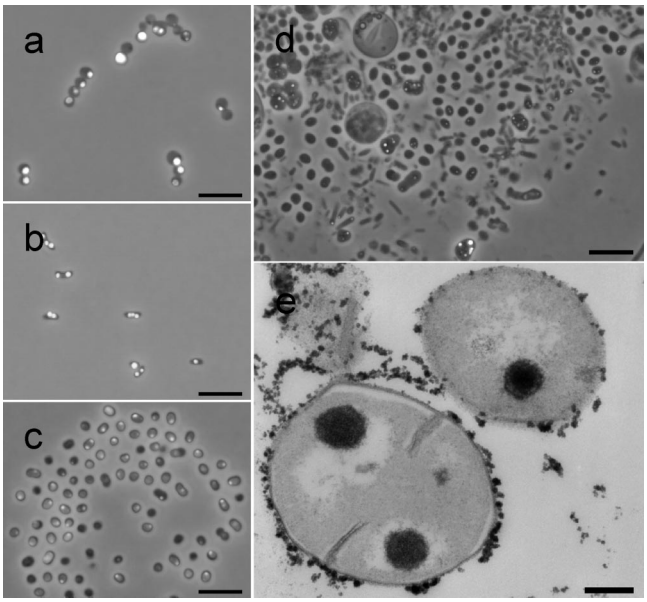

FIG. 1. (a to d) TC-stained cells of *M. phosphovorus* (a), the *Pseudomonas* sp. (b), the *Paracoccus* sp. (c), and activated sludge (d) harvested from the aerobic cultivation phase. For improved visualization of the polyphosphate granule distribution within the cells, the fluorescent images were merged with the respective light microscopic images. Bars, 5 μm. (e) Cells of *M. phosphovorus* stained for polyphosphates and analyzed by TEM. Bar, 0.2 μm.

Samples of *M. phosphovorus* taken from the aerobic phase contained 7.02% (±0.17%) green fluorescent cells, whereas only 1.07% (±0.08%) green fluorescent cells were found in samples from the anaerobic phase.

Several experiments were conducted to verify reliable, specific, and quantitative TC staining of cellular polyphosphate. First, DAPI, which is traditionally used for staining of polyphosphate granules in bacteria at a concentration range of 18 to 180 μM (see the introduction), was used for comparison. The dye was applied at a concentration of 28 μM to stain polyphosphate in aerobically grown *M. phosphovorus*. Flow cytometric analysis resulted in the detection of 8.34% (±0.32%) and 8.24% (±0.14%) polyphosphate-containing cells after DAPI and TC staining, respectively. Second, possible unspecific staining of cellular constituents by TC was tested using *Escherichia coli* K-12, a bacterium that does not produce polyphosphate granules (29). TC (0.225 mM) caused no fluorescence labeling of *E. coli* (0.03% ± 0.01%), whereas DAPI (28 μM) caused greenish fluorescence of 1.30% (±0.03%) of the treated cells. Third, *Methylobacterium rhodesianum* MB126 was used to test for possible binding of TC to PHB granules. The presence of PHB was verified using Nile red, which caused

bright red fluorescence, whereas TC caused no fluorescence with PHB (0.03% ± 0.01%). Eventually, the glycogen-accumulating species *M. glycogenica*, which does not produce polyphosphates, was also tested for green unspecific staining, but it showed no TC fluorescence (0.03% ± 0.01%).

Polyphosphate versus DNA staining in pure cultures. Analyzing the cytometric proliferation patterns of bacteria gives information about the growth rate of a species. As we were interested in the abundance and growth activity of PAOs, we combined the analysis of polyphosphate contents by TC staining with the analysis of growth activity based on DNA pattern analyses using DAPI (1 μM) by monitoring bacterial chromosome numbers. The results are presented in Fig. S5 in the supplemental material.

To simultaneously obtain information about growth activities and polyphosphate accumulation of individual cells in a population, it was important that the DAPI and the TC stains did not interfere. Indeed, reliable information on DNA pattern distributions was obtained with cells that had been exposed to TC prior to the addition of 1 μM DAPI solution. With this biphasic staining, it was intended that TC would bind to the polyphosphate granules before DAPI molecules would bind there. To detect possible influences of TC on the apparent distribution of the chromosome numbers, cells were stained with DAPI alone or in combination with TC. The DAPI fluorescence intensities and distributions of chromosome equivalents (in parentheses) obtained with DAPI only were as follows: C_{2n}, 12 (50%); C_{4n}, 24 (30%); C_{8n}, 47 (7%); and C_{xn}, 183 (13%) (Fig. 2a). With DAPI applied in combination with TC, the results were as follows: C_{2n}, 12 (50%); C_{4n}, 25 (30%); C_{8n}, 47 (7%); and C_{xn}, 179 (13%). The similarity shows that TC did not influence quantitative DNA staining with DAPI. The TC-stained cells (6.1%) were determined after gating and are shown as white dots in the DAPI-FSC plots (Fig. 2b). The polyphosphate-containing individuals were distributed over the entire population, but as a rule, the relative presence of polyphosphate-accumulating individuals was higher in subpopulations with more chromosome equivalents. The percentage decreased from 28.8% (C_{xn}) to 4.5% (C_{8n}), 3.3% (C_{4n}), and 9.3% (C_{2n}). C_{1n} cells were nearly not present within the sample, which corresponded to a state similar to that shown in Fig. S5b in the supplemental material, after 6 h cultivation.

When bacterial polyphosphate is stained with high concentrations of DAPI (28 μM), some of the dye also interacts with the DNA. We therefore checked whether DAPI staining alone could be used to infer both the DNA and the polyphosphate contents from the respective blue and yellow-green fluorescences. Using the same sample of *M. phosphovorus* as described above (see Fig. S6 in the supplemental material), the same fraction of polyphosphate-containing cells (6.2%) was found. Also, the previously observed four subpopulations based on chromosome equivalents were found and characterized by the same mean DAPI fluorescence intensity of each individual subcommunity as before. However, the apparent distribution of bacteria between these subcommunities was shifted toward higher fluorescence intensities as follows: C_{2n}, 13 (5%); C_{4n}, 26 (4%); C_{8n}, 55 (17%); and C_{xn}, 240 (74%). These results verified that the linkage of cell proliferation to polyphosphate synthesis using high DAPI concentrations alone was not reliable. Therefore, we strongly recommend application of the combined labeling approach involving DAPI at low concentration (1 μM) and TC (0.225 mM).

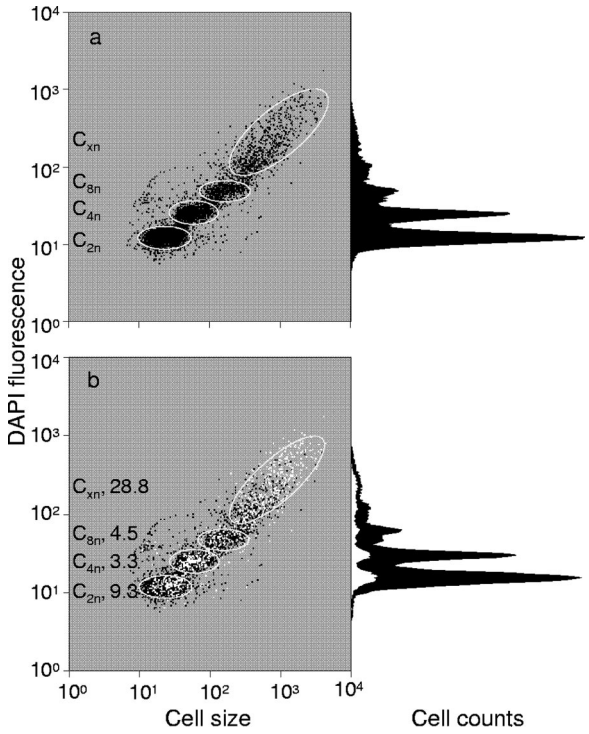

FIG. 2. Pattern of DNA distributions within a DAPI-stained culture (a) and a DAPI/TC-stained culture (b) of *M. phosphovorus*. DAPI-stained cells are shown in black. Prominent subpopulations characterized by distinct DNA contents are marked with gates (white ellipses). PAOs within the sample are marked with white dots in the dot plot and as a white area in the histogram; the percentage of the PAOs in subpopulations is given on the left side of panel b.

PAO dynamics in wastewater communities. The dual-staining technique was tested by analyzing PAO dynamics in activated sludge as a proof-of-principle study. The DAPI approach provides information on subcommunity abundance dynamics within natural communities, whereas the TC stain highlights polyphosphate-accumulating community members.

Activated sludge was cultivated in a sequenced batch mode and subjected to alternating aerobic and anaerobic growth conditions. Samples were harvested from both cultivation phases. Biomass was found to be produced at constant rates; sometimes floc formation was observed after several aerobic/anaerobic cycles. The MLSS, MLVSS, and ash contents did not change much during the bioreactor cultivation. We measured 3.0 (± 0.02) g liter^{-1} MLSS, 2.4 (± 0.00) g liter^{-1} MLVSS, and 0.6 (± 0.02) g liter^{-1} ash for the aerobic phase, compared to 2.7 (± 0.58) g liter^{-1} MLSS, 2.2 (± 0.41) g liter^{-1} MLVSS, and 0.5 (± 0.18) g liter^{-1} ash for the anaerobic phase. The nitrate concentration was close to zero during the anaerobic phases, indicating nitrate-reducing conditions (see Fig. S7 in the supplemental material). The stationary orthophosphate concentration was set to relatively high values up to nearly 180 mg liter^{-1} to stimulate the polyphosphate accumulation for convenient fluorescence visualization (Fig. 1d). Low phosphate concentrations as in the OECD medium (e.g., 15 mg liter^{-1}) led to fewer than 1% PAOs within the community. To visualize

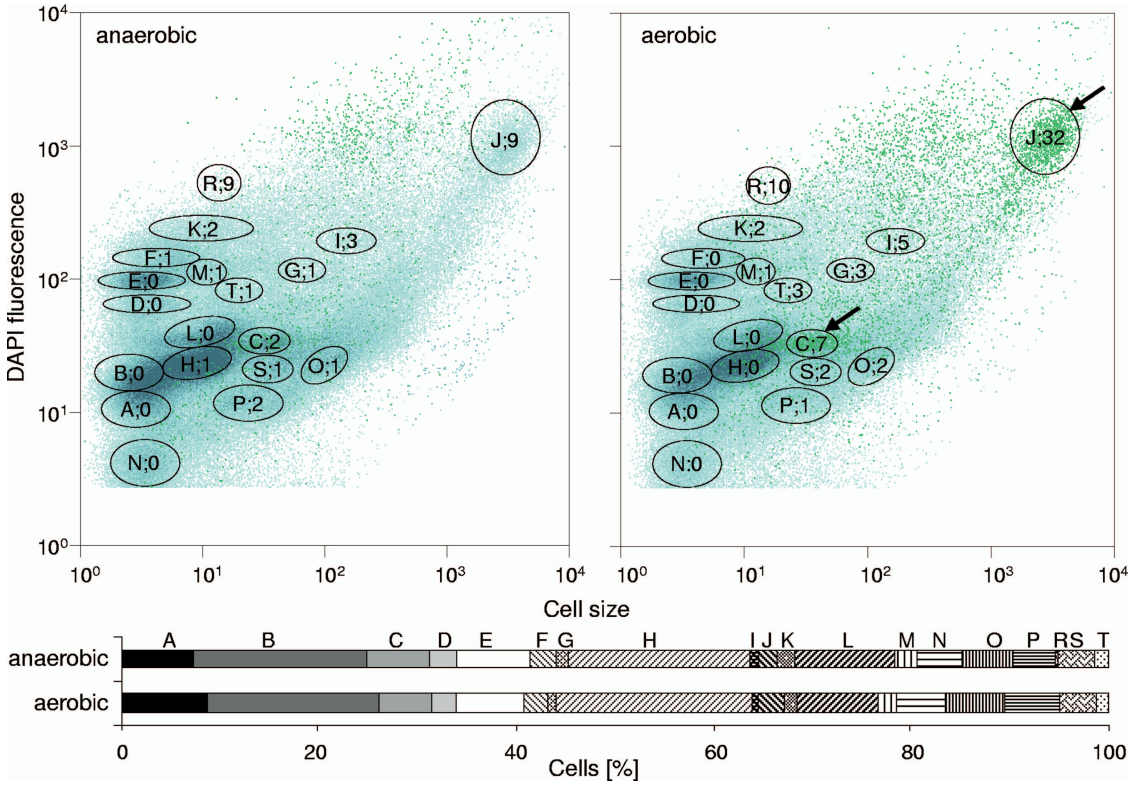

FIG. 3. Pattern of DNA distributions (blue, with dominant subcommunities marked with black gates) and PAO distribution (green dots and numbers within the gates [percent]) of cells harvested from the anaerobic and aerobic cultivation phases and double stained with DAPI and TC. Subcommunities with a high PAO content are marked with arrows. The amount of cells within each subcommunity is shown in the lower part as two bars for the respective cultivation phases.

changed polyphosphate granule accumulation during the anaerobic and aerobic phases, cells were harvested 5 min after entering the anaerobic phase and 105 min after entering the subsequent aerobic phase (158 mg orthophosphate liter^{-1} in this sample). They were fixed and stained with DAPI and TC. As expected, higher quantities of polyphosphate-containing cells were found during the aerobic cultivation phase (2.9%) (Fig. 3) than in the anaerobic phase (0.8%).

Within the same sample, up to 19 subcommunities differing in either polyphosphate or DNA contents as well as cell size were found. The bars at the bottom of Fig. 3 give their relative abundances. The numbers and letters in Fig. 3 indicate percentages of PAOs within the gates and the denomination of the subcommunities, respectively. It is remarkable that neither the number of distinct subcommunities nor the corresponding cell abundances changed much between the aerobic and anaerobic phases. However, it was striking that most PAOs were found in only few of the subcommunities in the sample from the aerobic phase. These PAOs were characterized by intermediate to high FSC and intermediate to high DNA contents. We never observed them to be members of the very small and low-DNA-content subcommunities at the left side of the histogram. The majority of the PAOs were present in two subcommunities (C and J), to which they contributed 7.3% and 32%, respectively. The sizes of the polyphosphate granules varied between 0.39 and 0.41 μm in diameter (Fig. 1d).

Additionally, the activated sludge cultivation regimen was modified by altering stationary orthophosphate and carbon concentrations to prove the effectiveness of the new PAO detection technique. PAO abundances were followed in dependence on stationary phosphate concentrations, increasing from 57 mg liter^{-1} (days I/Ia) to 74 mg liter^{-1} (days II/IIa), 97 mg liter^{-1} (days IV/IVa), 151 mg liter^{-1} (days V/Va), and 158 mg liter^{-1} (day III) (Fig. 4) in combination with elevated carbon contents from 583 mg liter^{-1} (days I/Ia, II/IIa, and III) to 1,166 mg liter^{-1} (days IV/IVa and V/Va). Samples were taken in duplicate during the aerobic phases only, on different days separated by several shifts of the oxygen regimen. As a result, increased phosphate concentrations clearly led to increased fractions of PAOs within the sludge, from about 0.3% with 57 mg phosphate liter^{-1} to 4% with 151 mg phosphate liter^{-1}. Otherwise, the relative abundances of bacterial cells in the 19 predefined subcommunities remained nearly unchanged during the cultivation on 583 mg liter^{-1} carbon. Seven major subcommunities (A, B, C, E, H, L, and N; each above 5%) comprised nearly 80% of the whole community. When the carbon concentration was doubled to 1,165 mg liter^{-1} COD, a different distribution of the community's individuals developed. Although the total number of the distinguishable 19 subcommunities remained constant, changed dominance patterns were observed. Now 11 main subcommunities (A, B, C, D, E, G, H, N, P, S, and T; each above 5%) comprised 90% of all cells in the 19 subcommunities. This shows the massive influence of the carbon concentration on the community struc-

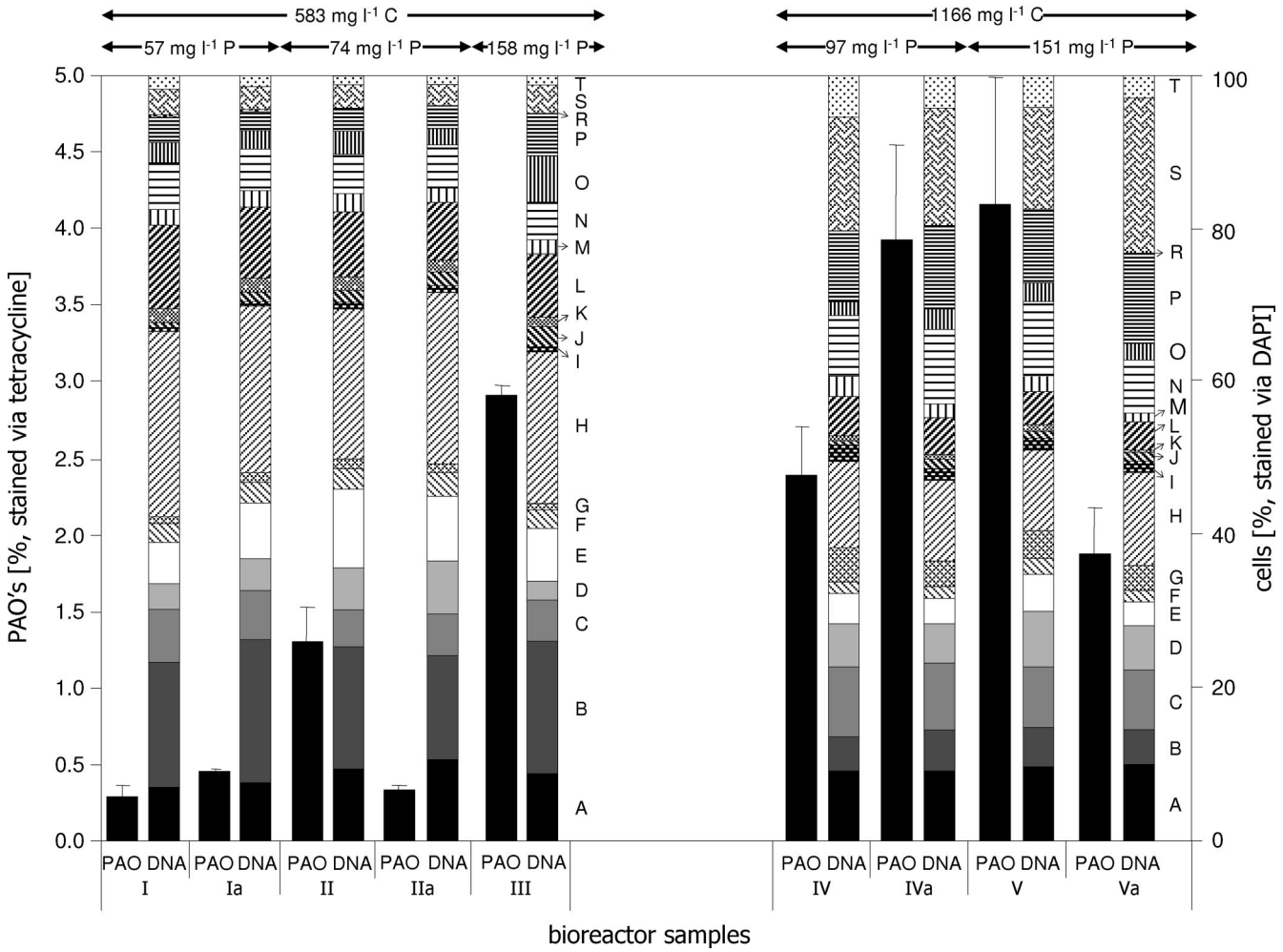

FIG. 4. DNA pattern (right panel; labels correspond to those in Fig. 3) and proportions of PAOs (left panel) of an activated sludge community cultivated in the SBR for 32 days. The cells were harvested from the aerobic cultivation phase and double stained with DAPI and TC. Phosphorous and carbon concentrations were varied as indicated at the top.

ture. Nevertheless, the general abundances of the key PAO-containing subcommunities C and J stayed nearly constant during cultivation on low carbon concentrations, with J slightly increasing in cell number. A similar stability was observed with higher carbon concentrations, although the abundance of C increased from 6 to 9%, whereas cell numbers in J slightly decreased to 2%. Hence, PAO abundances and dynamics of key subcommunities were effectively detected, which seems to depend on stationary orthophosphate concentrations in the first place, whereas the changing carbon concentrations surely alter the overall cell abundances within the subcommunities.

Phylogenetic affiliation of PAOs in WWTPs. The reliability of the dual-labeling technique was also tested by analyzing a sample harvested from an aeration tank of an industrial WWTP with an orthophosphate concentration of 15 mg liter^{-1}. The sample was aerated and kept on ice until flow cytometric analysis. TC staining revealed that 10.2% of the cells contained polyphosphate granules. Plotting DNA contents (DAPI) against cells size (FSC) revealed 13 distinct subcommunities, 8 of which contributed to more than 5% each and summed up to 85% of all cells in the 13 subcommunities. The polyphosphate-positive cells were sorted and subjected to DNA extraction for the phylogenetic identification of PAOs.

A 16S rRNA gene clone library of 78 clones was generated and screened by amplified rRNA gene restriction analysis. Based on different restriction patterns, 43 representative clones were partially sequenced. Phylogenetic affiliations of the sequences based on the RDP taxonomy and the highest BLAST hit are given in Table 2. The most frequent phylotype, comprising 27 clones, was affiliated with the *Rhodocyclaceae*. These sequences showed high similarity to clones retrieved from EBPR sludge, among them those affiliated to the "*Candidatus* Accumulibacter" lineage (13). The second most frequent phylotype, with 13 clones, was assigned to the genus *Pseudomonas*. A third group, comprising seven clones, was a phylotype belonging to the *Gammaproteobacteria* and related to glycogen-accumulating organisms retrieved from an EBPR WWTP (accession no. DQ201885). A phylotype assigned to the genus *Nitrospira* was also represented by seven clones. Four clones were assigned to the genus *Tetrasphaera* and closely related to actinobacterial PAOs detected in an EBPR plant (20). The genus *Dechloromonas* was also represented by four

TABLE 2. Results of sequencing of representative 16S rRNA gene clones

Clone	Accession no.	Highest BLAST hit (accession no.)/% identity	Taxonomic affiliation according to RDP
B3 (471)	EU850359	Uncultured betaproteobacterium clone S7 (AF447793)/98	*Rhodocyclaceae*
C10 (475)	EU850366	Uncultured betaproteobacterium clone nsc151 (DQ211501)/100	*Rhodocyclaceae*
C11 (501)	EU850367	Uncultured bacterium SA34 (AF245349)/99	*Rhodocyclaceae*
D7 (525)	EU850371	Uncultured bacterium clone UTFS-002-12-23 (AB166771)/99	*Rhodocyclaceae*
D10 (483)	EU850372	Uncultured bacterium clone UTFS-002-12-23 (AB166771)/99	*Rhodocyclaceae*
E3 (468)	EU850376	Uncultured bacterium SA34 (AF245349)/99	*Rhodocyclaceae*
E4 (477)	EU850377	Uncultured bacterium clone VIR_D5 (EF565151)/99	*Rhodocyclaceae*
E6 (458)	EU850379	Uncultured bacterium clone VIR_D5 (EF565151)/99	*Rhodocyclaceae*
E8 (516)	EU850381	Uncultured bacterium SA34 (AF245349)/98	*Rhodocyclaceae*
F5 (497)	EU850384	Uncultured bacterium clone UTFS-002-12-23 (AB166771)/99	*Rhodocyclaceae*
F11 (485)	EU850389	Uncultured bacterium clone VIR_D5 (EF565151)/98	*Rhodocyclaceae*
H5 (512)	EU850394	Uncultured bacterium clone D07 (EF589969)/97	*Rhodocyclaceae*
OTU[a] 1		27 clones	*Rhodocyclaceae*
A1 (425)	EU850352	*Pseudomonas putida* KT2440 (AE015451)/99	*Pseudomonas* spp.
E5 (443)	EU850378	*Pseudomonas putida* isolate 24 (EU438854)/99	*Pseudomonas* spp.
E12 (515)	EU850383	*Pseudomonas putida* BM2 (DQ989291)/99	*Pseudomonas* spp.
OTU 2		13 clones	*Pseudomonas* spp.
B1 (291)	EU850358	Uncultured *Nitrospira* sp. clone 0B11 (EU499597)/98	*Nitrospira* spp.
B8 (578)	EU850362	Uncultured *Nitrospira* sp. clone 3 (DQ414437)/99	*Nitrospira* spp.
E2 (463)	EU850375	Uncultured *Nitrospira* sp. clone 3 (DQ414437)/99	*Nitrospira* spp.
OTU 3		7 clones	*Nitrospira* spp.
A2 (407)	EU850353	Uncultured gammaproteobacterium clone GB2917y (DQ201885)/96	*Gammaproteobacteria*
A5 (389)	EU850355	Uncultured gammaproteobacterium clone GB2917y (DQ201885)/95	*Gammaproteobacteria*
A7 (477)	EU850357	Uncultured gammaproteobacterium clone GB2917y (DQ201885)/94	*Gammaproteobacteria*
OTU 4		7 clones	*Gammaproteobacteria*
A3 (485)	EU850354	Uncultured eubacterium clone F13.46 (AF495440)/98	*Tetrasphaera* spp.
E9 (451)	EU850382	Uncultured bacterium clone Ebpr19 (AF255629)/99	*Tetrasphaera* spp.
F9 (473)	EU850387	Uncultured eubacterium clone F13.46 (AF495440)/98	*Tetrasphaera* spp.
OTU 5		4 clones	*Tetrasphaera* spp.
A6 (447)	EU850356	*Dechloromonas* sp. strain A34 (EF632559)/97	*Dechloromonas* spp.
D11 (504bp)	EU850373	Uncultured bacterium clone ORS10C_g11 (EF392932)/99	*Dechloromonas* spp.
E7 (535)	EU850380	*Dechloromonas* sp. strain A34 (EF632559)/97	*Dechloromonas* spp.
OTU 6		4 clones	*Dechloromonas* spp.
B7 (448)	EU850361	Uncultured actinobacterium clone DOK_NOFERT_clone341 (DQ829293)/96	*Actinomycetales*
F8 (450)	EU850386	Uncultured actinobacterium clone DOK_NOFERT_clone341 (DQ829293)/96	*Actinomycetales*
OTU 7		2 clones	*Actinomycetales*
E1 (438)	EU850374	Uncultured bacterium clone T015D (AM158382)/91	Candidate division TM7
H2 (428)	EU850393	Uncultured bacterium clone IC-61 (AB255073)/93	Candidate division TM7
OTU 8		2 clones	Candidate division TM7
C12 (530)	EU850368	Uncultured bacterium clone DSSD59 (AY328757)/98	*Alphaproteobacteria*
G12 (559)	EU850392	*Derxia gummosa* (AB089482)/95	*Betaproteobacteria*
C2 (413)	EU850365	Uncultured bacterium clone 197up (AY212650)/99	*Burkholderiales*
B10 (532)	EU850363	*Ralstonia detusculanense* (AF280433)/99	*Ralstonia* spp.
D1 (452)	EU850369	Uncultured bacterium clone TH-141 (AB184983)/98	*Comamonadaceae*
F7 (457)	EU850385	Uncultured bacterium clone 44 (DQ413103)/99	*Rhodocyclaceae*
G10 (449)	EU850391	Uncultured bacterium clone SRRB48 (AB240518)/96	*Nocardioidaceae*
B5 (458)	EU850360	Uncultured *Sphingobacteria* bacterium clone ADK-SGe02-50 (EF520599)/96	*Sphingobacteriales*
B11 (522)	EU850364	Uncultured bacterium clone HM15 (AM909923)/95	*Acidobacteriaceae*
F10 (495)	EU850388	Uncultured bacterium clone LaP15L89 (EF667686)/99	*Caldilinea* spp.
D5 (435)	EU850370	Uncultured bacterium clone mdt16a02 (AY537009)/98	*Bacteria*
F12 (574)	EU850390	Uncultured bacterium clone 032D06_P_BA_P3 (BX294877)/92	*Bacteria*

[a] OTU, operational taxonomic unit.

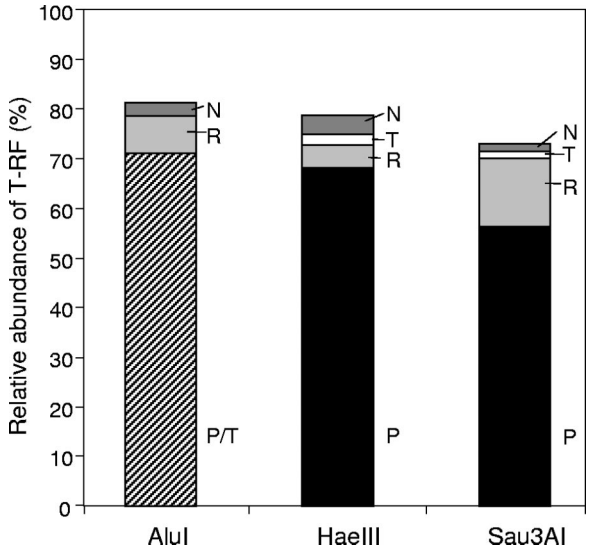

FIG. 5. Relative abundances of T-RF after digestion with the restriction endonucleases AluI, HaeIII, and Sau3AI. The T-RF values were assigned to phylotypes according to the experimentally determined T-RF values of the respective clones. P, *Pseudomonas* spp.; R, *Rhodocyclaceae*; T, *Tetrasphaera* spp.; N, *Nitrospira* spp. With AluI, the T-RF values of *Pseudomonas* spp. and *Tetrasphaera* spp. were identical, and therefore their relative abundances are summarized.

clones. Other phylotypes present in minor proportions were affiliated with another group of the *Actinomycetales* (two clones) and the candidate division TM7 (two clones), and 12 other phylotypes were represented only by single clones (Table 2).

T-RFLP analysis revealed that, in contrast to the results from the clone library, the T-RF assigned to *Pseudomonas* spp. was most frequent, comprising more than 50% of the total peak area (Fig. 5). The *Rhodocyclaceae* phylotype related to "*Candidatus* Accumulibacter" as well as the *Tetrasphaera*- and *Nitrospira*-like phylotypes were also detected in the T-RFLP profiles but with lower percentages than expected from the clone library. These results indicate that *Pseudomonas* spp. are the predominant polyphosphate-containing PAOs in the EBPR community analyzed here.

DISCUSSION

Determination and quantification of PAOs in highly diverse bacterial communities such as activated sludge are of high interest because of the need for improved phosphorus removal from domestic wastewater. Scientists and practitioners today are aware that the community members actually involved in the biological removal of phosphorus in wastewater are often unrelated to laboratory strains known to accumulate phosphate. Furthermore, many wastewater microorganisms have the capacity to accumulate the energy-rich compound but do not do so, for reasons not fully understood. Cultivation-independent and quantitative diagnosis of polyphosphate-containing PAOs is therefore a powerful tool to gain a complete overview and sound basis for the development of process strategies making the process more reliable.

In this paper the antibiotic TC was proven to show highly polyphosphate-specific and stable fluorescence. The specificity for polyphosphate granules was tested with known PAOs such as *M. phosphovorus*, the *Paracoccus* sp., and the *Pseudomonas* sp. as well as against a non-phosphate-accumulating strain of *E. coli*, the glycogen-producing strain *M. glycogenica* Lg2^T, and a strongly PHB-accumulating strain of *M. rhodesianum*. We compared the new in vivo TC staining method with the traditional DAPI method and found them to be comparable in terms of the numbers of labeled cells and the fluorescence intensities of their phosphate granules. However, the TC stain proved to be superior to the DAPI stain due to a 15-times-lower unspecific background labeling. This was regardless of the fact that the TC fluorescence originates from the strong chelation of divalent cations, which are present not only in polyphosphate granules but also in the cell wall, protein complexes, and the cytoplasm (5, 38). Endospores of spore-forming bacteria such as *Bacillus subtilis* which do contain calcium ions also did not show any TC fluorescence above the autofluorescence level (not shown). The TC binding to polyphosphate inside living cells of *M. phosphovorus* and an activated sludge community was found to be very stable. Although nearly 40 different efflux systems have been described in various strains to protect the aminoacyl-tRNA binding sites of bacterial ribosomes against the action of TC, we found no sign of TC efflux. TC molecules strongly chelate with divalent cations. This allows them to enter various bacterial species driven by the cells' Donnan potential across the outer membrane that acts on the cations (6). In the periplasm the slightly lipophilic TC molecules are then liberated and diffuse in the cytoplasm.

A very important advantage of TC as opposed to DAPI staining of polyphosphate was the possibility to combine it with DNA analysis. Staining of the bacterial DNA gives information on bacterial growth rates (26, 28) and therefore on activity states of PAOs when analyzed in combination with TC. DAPI staining alone of both DNA and polyphosphate granules did not result in a reliable analysis of the two characteristics. However, the dual stain with TC and DAPI proved to be a quantitative method for PAO detection and DNA content analysis.

We were able to detect polyphosphate-bearing microorganisms even when they contributed less than 1% to a pure culture or a wastewater community. Since the abundances of PAOs are of great interest for EBPR processes, we propose the use of our technique for quick and reliable authentication of PAOs in WWTPs. Traditional models imply that polyphosphate accumulation occurs during aerobic growth or if the cells are exposed to stress situations such as the decrease of external pH or carbon substrate concentration (2). However, recent studies showed that some species still keep polyphosphate granules even under anaerobic conditions (36). Also, it is now known that other species which long have served as indicator organisms for polyphosphate accumulation do not reliably accumulate polyphosphates under aerobic conditions in the WWTP process stages (13, 46). For instance, organisms possessing the *ppk* gene, which encodes the main enzyme involved in the synthesis of polyphosphate granules, do not always contain granules in a WWTP regardless of the oxygen regimen (e.g., *E. coli* [30]). Another possible way to approach PAOs in an EBPR process is the application of oligonucleotide FISH probes specific for phylogenetic groups that are known as PAOs. However, these organisms do not always produce polyphosphates

and might have such low rRNA contents that they cannot be detected by conventional FISH techniques. The more sensitive catalyzed reporter deposition-FISH technique destroys the structural integrity of the cells, thereby making them unsuitable for flow cytometry. Activity-based techniques such as microautoradiography-FISH have been applied successfully to detect PAOs (17). However, for routine in situ monitoring of active PAO populations in industrial WWTPs, our fluorescence-based approach using simple and reliable staining techniques and flow cytometry as a quick analytical tool appears more suitable. Moreover, unlike FISH techniques, it also includes PAOs of unknown phylogeny.

Within natural communities PAO determination was possible using the dual-stain technique. Moreover, we found 19 subcommunities according to DNA versus FSC characteristics, which is an extremely high community resolution when investigating bacterial communities by flow cytometry. This resolution may also hint at a highly diverse culture. Additionally, the DNA/TC patterns revealed information on key PAO subcommunity dynamics. It appears justified to conclude that an increase in bacterial cell number within every subcommunity is caused by cell proliferation and upcoming new cell types (19). Such an approach based on DNA pattern analysis combined with the detection of TC-labeled polyphosphates can be regarded as highly reliable and quantitative, since there is no risk of active dye excretion by fixed cells (26, 43).

In fact, the bioreactor experiments combined with the dual-staining technique revealed high qualitative and quantitative community stability through aerobic and anaerobic cultivation modes. This behavior seems to be typical for activated sludge communities, as previously shown by bulk single-strand conformation polymorphism analysis (45). The doubled substrate concentration had a higher influence and changed the structure of the community, as was seen by altered abundances in the 19 subcommunities. It is known that high community diversity is a prerequisite for high resilience, as diverse communities can flexibly react to environmental fluctuations because of the ecological complementarity of functionally redundant groups. This has been demonstrated particularly in wastewater and activated sludge communities (17, 30). Future phylogenetic allocation of the upcoming species within the respective subcommunities can be performed using cell sorting as an approach which was already reliably applied (19).

Therefore, the application of the dual stain to wastewater communities enabled differentiation of the entire, complex community into subcommunities that largely differed in their growth rates and their polyphosphate contents. The dynamics of these subcommunities were followed according to cell numbers and polyphosphate contents. This was the desired basis for the separation of the actively polyphosphate-accumulating organisms from the activated sludge community for phylogenetic analysis. The results of 16S rRNA gene sequencing verified the specificity of the staining technique, as the clone library generated from separated subcommunities displayed a rather low diversity and was composed basically of phylotypes known as PAOs, such as the "*Candidatus* Accumulibacter"-like phylotype, members of the genus *Pseudomonas*, and the *Tetrasphaera*-related actinobacteria. Although the clone library probably does not reflect the complete phylogenetic spectrum present in the sorted subcommunity, as indicated by several unique clones, its composition confirms that predominantly PAOs were captured. Moreover, T-RFLP profiles revealed the predominance of a single phylotype belonging to the genus *Pseudomonas*. Surprisingly, this phylotype was only the second-most one in the clone library, but T-RFLP profiles recorded with three different restriction enzymes clearly showed the predominance of this sequence type. This bias might be explained by the low coverage of the clone library that led to an underestimation of the *Pseudomonas* sequence type. On the other hand, the relative T-RF peak areas might overestimate the relative abundances of the corresponding phylotypes, as sequence types without restriction sites within the 35- to 650-bp threshold are not considered and therefore not included in the total peak area. Nevertheless, sequencing and T-RFLP profiling of 16S rRNA genes verified that PAOs were specifically detected and captured out of a complex community. Thus, the TC dual-staining approach in combination with high-throughput techniques such as T-RFLP fingerprinting enables the quick and reliable detection and quantification of distinct PAO groups. In contrast to the FISH technique, it can also detect PAOs of not-yet-known phylogenetic affiliation. Our primary goal to quickly detect PAOs and to make them available for identification as a basis for the improvement of EBPR processes was therefore achieved.

In summary, we have developed a dual-stain technique to reliably quantify PAOs and relate them to growth activities within activated sludge communities in WWTPs. DAPI and TC are inexpensive dyes that do not change the features of the cells and can be applied quickly and without complicated sample handling. The procedure is easy to perform, quick, and cultivation independent. In the future we aim to combine this technique with phylogenetic analyses to give an on-line tool for monitoring EBPR stability and forming a basis for the optimization of process control.

ACKNOWLEDGMENTS

We thank H. Engewald, C. Süring, U. Lohse, and S. Jahn for technical assistance in the laboratory. We thank also W. Geyer for the use of the fluorescence spectrophotometer and M. Eschenhagen for analysis of the COD, nitrate, and orthophosphate values of the WWTP sample.

This work was supported by the German Federal Ministry of Education and Research (no. 02WA0700).

REFERENCES

1. **Ackermann, J. U., S. Müller, A. Lösche, T. Bley, and W. Babel.** 1995. *Methylobacterium rhodesianum* cells tend to double the DNA content under growth limitations and accumulate PHB. J. Biotechnol. **39:**9–20.
2. **Ahn, J., S. Schroeder, M. Beer, S. McIlroy, R. C. Bayly, J. W. May, G. Vasiliadis, and R. J. Seviour.** 2007. Ecology of the microbial community removing phosphate from wastewater under continuously aerobic conditions in a sequencing batch reactor. Appl. Environ. Microbiol. **73:**2257–2270.
3. **Altschul, S. F., W. Gish, W. Miller, E. W. Myers, and D. J. Lipman.** 1990. Basic local alignment search tool. J. Mol. Biol. **215:**403–410.
4. **Ault-Riche, D., C. D. Fraley, C. M. Tzeng, and A. Kornberg.** 1998. Novel assay reveals multiple pathways regulating stress-induced accumulations of inorganic polyphosphate in *Escherichia coli*. J. Bacteriol. **180:**1841–1847.
5. **Chang, C.-F., H. Shuman, and A. P. Somlyo.** 1986. Electron probe analysis, X-ray mapping, and electron energy-loss spectroscopy of calcium, magnesium, and monovalent ions in log-phase and in dividing *Escherichia coli* B cells. J. Bacteriol. **167:**935–939.
6. **Chopra, I., and M. Roberts.** 2001. Tetracycline antibiotics: mode of action, applications, molecular biology, and epidemiology of bacterial resistance. Microbiol. Mol. Biol. Rev. **65:**232–260.
7. **Clesceri, L. S., A. E. Greenberg, and A. D. Eaton.** 1998. Standard methods for the examination of water and wastewater, 20th ed. American Public Health Association, Washington, DC.

8. **Cloete, T. E., and P. L. Steyn.** 1987. A combined fluorescent antibody membrane filter technique for enumerating Acinetobacter in activated sludges, p. 335–338. *In* R. Ramadori (ed.), Biological phosphate removal from wastewater. Pergamon, Oxford, United Kingdom.
9. **Cole, J. R., B. Chai, R. J. Farris, Q. Wang, A. S. Kulam-Syed-Mohideen, D. M. McGarrell, A. M. Bandela, E. Cardenas, G. M. Garrity, and J. M. Tiedje.** 2007. The ribosomal database project (RDP-II): introducing *myRDP* space and quality controlled public data. Nucleic Acids Res. **35**(database issue)**:**D169–D172. doi:10.1093/nar/gkl889.

9a. **Eaton, A. D., L. S. Clesceri, and A. E. Greenberg.** 1995. Standard methods for the examination of water and wastewater, 19th ed. American Public Health Association, Washington, DC.

10. **Garcia Martin, H., N. Ivanova, V. Kunin, F. Warnecke, K. W. Barry, A. C. McHardy, C. Yeates, S. He, A. A. Salamov, E. Szeto, E. Dalin, N. H. Putnam, H. J. Shapiro, J. L. Pangilinan, I. Rigoutsos, N. C. Kyrpides, L. L. Blackall, K. D. McMahon, and P. Hugenholtz.** 2006. Metagenomic analysis of two enhanced biological phosphorus removal (EBPR) sludge communities. Nat. Biotechnol. **24:**1263–1269.
11. **Günther, S., T. Hübschmann, M. Rudolf, M. Eschenhagen, I. Röske, H. Harms, and S. Müller.** 2008. Fixation procedures for flow cytometric analysis of environmental bacteria. J. Microbiol. Methods **75:**127–134.
12. **Hallett, M., A. S. Schneider, and E. Carbone.** 1972. Tetracycline fluorescence as calcium-probe for nerve membrane with some model studies using erythrocyte ghosts. J. Membr. Biol. **10:**31–44.
13. **He, S., D. L. Gall, and K. D. McMahon.** 2007. "*Candidatus* Accumulibacter" population structure in enhanced biological phosphorus removal sludges as revealed by polyphosphate kinase genes. Appl. Environ. Microbiol. **73:**5865–5874.
14. **Hrenovic, J., D. Tibljaš, H. Büyükgüngör, and Y. Orhan.** 2003. Influence of support materials on phosphate removal by the pure culture of *Acinetobacter calcoaceticus*. Food Technol. Biotechnol. **41:**331–338.
15. **Jensen, T. E.** 1968. Electron microscopy of polyphosphate bodies in a blue-green algae, *Nostoc pruniforme*. Arch. Microbiol. **62:**144–152.
16. **Kawaharasaki, M., H. Tanaka, T. Kanagawa, and K. Nakamura.** 1999. *In situ* identification of polyphosphate-accumulating bacteria in activated sludge by dual staining with rRNA-targeted oligonucleotide probes and 4′,6-diamidino-2-phenylindol (DAPI) at a polyphosphate-probing concentration. Water Res. **33:**257–265.
17. **Kindaichi, T., T. Ito, and S. Okabe.** 2004. Ecophysiological interaction between nitrifying bacteria and heterotrophic bacteria in autotrophic nitrifying biofilms as determined by microautoradiography-fluorescence in situ hybridization. Appl. Environ. Microbiol. **70:**1641–1650.
18. **Klauth, P., S. R. Pallerla, D. Vidaurre, C. Ralfs, V. F. Wendisch, and S. M. Schoberth.** 2006. Determination of soluble and granular inorganic polyphosphate in *Corynebacterium glutamicum*. Appl. Microbiol. Biotechnol. **72:**1099–1106.
19. **Kleinsteuber, S., V. Riis, I. Fetzer, H. Harms, and S. Müller.** 2006. Population dynamics of a microbial consortium during growth on diesel fuel in saline environments. Appl. Environ. Microbiol. **72:**3531–3542.
20. **Kong, Y., J. L. Nielsen, and P. H. Nielsen.** 2005. Identity and ecophysiology of uncultured actinobacterial polyphosphate-accumulating organisms in full-scale enhanced biological phosphorus removal plants. Appl. Environ. Microbiol. **71:**4076–4085.
21. **Kulaev, I., and T. Kulakovskaya.** 2000. Polyphosphate and phosphate pump. Annu. Rev. Microbiol. **54:**709–734.
22. **Lane, D. J.** 1991. 16S/23S rRNA sequencing, p. 115–175. *In* E. Stackebrandt and M. Goodfellow (ed.), Nucleic acid techniques in bacterial systematics. Wiley, Chichester, United Kingdom.
23. **Lee, T. C., S. Mohsin, D. Taylor, R. Parkesh, T. Gunnlaugsson, F. J. O'Brien, M. Giehl, and W. Gowin.** 2003. Detecting microdamage in bone. J. Anat. **203:**161–172.
24. **Liebermann, L.** 1888. Über das Nuclein der Hefe und künstliche Darstellung eines Nucleins aus Eiweiss und Metaphosphorsäure. Ber. Dtsch. Chem. Ges. **21:**598–600.
25. **Meistrich, M. L., W. Göhde, R. A. White, and J. Schumann.** 1978. Resolution of X and Y spermatids by pulse cytophotometry. Nature **274:**821–823.
26. **Müller, S.** 2007. Modes of cytometric bacterial DNA pattern: a tool for pursuing growth. Cell Prolif. **40:**621–639.
27. **Nelson, M. L.** 1998. Chemical and biological dynamics of tetracyclines. Adv. Dent. Res. **12:**5–11.
28. **Pawelczyk, S., W. R. Abraham, H. Harms, and S. Müller.** 2008. Community-based degradation of 4-chorosalicylate tracked on the single cell level. J. Microbiol. Methods **75:**117–126.
29. **Rao, N. N., M. R. Roberts, and A. Torriani.** 1985. Amount and chain length of polyphosphates in *Escherichia coli* depend on cell growth conditions. J. Bacteriol. **162:**242–247.
30. **Reid, N. M., T. H. Bowers, and G. Lloyd-Jones.** 2008. Bacterial community composition of a waste water treatment system reliant on N_2 fixation. Appl. Microbiol. Biotechnol. **79:**285–292.
31. **Röske, I., H.-D. Bauer, and D. Uhlmann.** 1989. Nachweis phosphorspeichernder Bakterien im Belebtschlamm mittels Elektronenmikroskopie und Röntgenspektroskopie. GWF Wasser Abwasser **130:**73–75.
32. **Saito, K., R. Ohtomo, Y. Kuga-Uetake, T. Aono, and M. Saito.** 2005. Direct labeling of polyphosphate at the ultrastructural level in *Saccharomyces cerevisiae* by using the affinity of the polyphosphate binding domain of *Escherichia coli* exopolyphosphatase. Appl. Environ. Microbiol. **71:**5692–5701.
33. **Santos, M. M., P. C. Lemos, M. A. M. Reis, and H. Santos.** 1999. Glucose metabolism and kinetics of phosphorus removal by fermentative bacterium *Microlunatus phosphovorus*. Appl. Environ. Microbiol. **65:**3920–3928.
34. **Serafim, L. S., P. C. Lemos, C. Levantesi, V. Tandoi, H. Santos, and M. A. Reis.** 2002. Methods for detection and visualization of intracellular polymers stored by polyphosphate-accumulating microorganisms. J. Microbiol. Methods. **51:**1–18.
35. **Seviour, R. J., T. Mino, and M. Onuki.** 2003. The microbiology of biological phosphorus removal in activated sludge systems. FEMS Microbiol. Rev. **27:**99–127.
36. **Shi, H.-P., and C.-M. Lee.** 2006. Combining anoxic denitrifying ability with aerobic-anoxic phosphorus-removal examinations to screen denitrifying phosphorus-removing bacteria. Int. Biodeterior. Biodegradation **57:**121–128.
37. **Shintani, T., W. T. Liu, S. Hanada, Y. Kamagata, S. Miyaoka, T. Suzuk, and K. Nakamura.** 2000. *Micropruina glycogenica* gen. nov., sp. nov., a new Gram-positive glycogen-accumulating bacterium isolated from activated sludge. Int. J. Syst. Evol. Microbiol. **50:**201–207.
38. **Smith, R. J.** 1995. Calcium and bacteria. Adv. Microb. Physiol. **37:**83–133.
39. **Spurr, A. R.** 1969. A low-viscosity epoxy resin embedding medium for electron microscopy. J. Ultrastruct. Res. **26:**31–43.
40. **Streichan, M., J. R. Golecki, and G. Schön.** 1990. Polyphosphate accumulating bacteria from sewage plants with different processes for biological phosphorus removal. FEMS Microbiol. Ecol. **73:**113–124.
41. **Tijssen, J. P. F., H. W. Beekes, and J. Van Steveninck.** 1982. Localization of polyphosphates in *Saccharomyces fragilis*, as revealed by 4′6-diamidino-2-phenylindole fluorescence. Biochim. Biophys. Acta **721:**394–398.
42. **van Groenestijn, J. W., G. J. F. M. Vlekke, D. M. E. Anink, M. H. Deinema, and A. J. B. Zehnder.** 1988. Role of cations in accumulation and release of phosphate by *Acinetobacter* strain 210A. Appl. Environ. Microbiol. **54:**2894–2901.
43. **Vogt, C., A. Lösche, S. Kleinsteuber, and S. Müller.** 2005. Population profiles of a binary bacterial culture grown with toluene under sulphate reducing conditions. Cytometry **66A:**91–102.
44. **Wagner, M., R. Erhart, W. Manz, R. Amann, H. Lemmer, D. Wedi, and K. H. Schleifer.** 1994. Development of an rRNA-targeted oligonucleotide probe specific for the genus *Acinetobacter* and its application for in situ monitoring in activated sludge. Appl. Environ. Microbiol. **60:**792–800.
45. **Zhao, Y. G., A. J. Wang, N. Q. Ren, and Y. Zhao.** 2008. Microbial community structure in different waste water treatment processes characterized by single-strand conformation polymorphism (SSCP) technique. Front. Environ. Sci. Engin. **2:**116–121.
46. **Zilles, J. L., C. H. Hung, and D. R. Noguera.** 2002. Presence of *Rhodocyclus* in a full-scale waste water treatment plant and their participation in enhanced biological phosphorus removal. Water Sci. Technol. **46:**123–128.